

# The Influence of Wall Conductivity on Flame Thermoacoustics in Rectangular Channels

Zachary T. Negrette and Scott I. Jackson  
Department of Aerospace Engineering  
Texas A&M University  
College Station, TX USA

Mark Short  
Shock and Detonation Physics Group  
Los Alamos National Laboratory  
Los Alamos, NM, USA

## 1 Introduction

Flames propagating in channels with widths approaching the reaction zone length can be significantly affected by heat loss from the flame to the channel walls. A commonly observed effect of heat loss is quenching, but heat transfer to the wall can also significantly impact flame propagation above this limit. The flame velocity can also vary significantly with channel width and equivalence ratio [1, 2]. These effects can be important for devices such as flame arresters and microcombustors [3, 4].

Thermoacoustic instabilities have been observed as pressure and flame-speed oscillations in narrow channels [5–8]. In calculations with viscous (but not thermal) losses, Gonzalez et al. [8] observed that the velocity of the unburned gases exhibited damped acoustic-strength oscillations. These were attributed to a decrease in the flame surface area and heat release when the flame was locally extinguished near the walls. The numerical studies of Jimenéz et al. [5, 6] are most similar with the present experiments. They [5] explored symmetric and asymmetric flame shapes perturbed by acoustic waves traveling in channels of variable width and length while modeling viscous effects at the wall. It was reported that the oscillatory dynamics depend on channel width, length, flame shape, and symmetry. Flames with symmetric shapes generally exhibited higher amplitude oscillations than asymmetric flames. They also found that these instabilities were quickly damped once the channel was reduced below a critical width or length. Additionally, they noted that increasing the channel length resulted in stronger self-sustained acoustic oscillations for both the symmetric and asymmetric flames. The oscillation frequencies closely agreed with the acoustic eigenmodes of the channel, which were modulated by the channel length and reactant and product gas properties [5]. The symmetric and asymmetric flames propagated with different speeds, oscillation frequencies, and oscillation amplitudes. Later, Jimenéz and Kurdyumov [6] added heat losses to the confining boundaries. They found that in some channels, flames that were typically asymmetric for adiabatic walls became symmetric after introducing heat losses. They concluded that the addition of heat losses led to the stabilization of the symmetric flame shape. Moreover, small amounts

of heat losses were found to increase the amplitude of the pressure oscillations. However, significantly increasing the heat loss had adverse effects on the oscillations and damped the thermoacoustic response.

While many have explored the flame-quenching phenomenon, there are few experimental studies performed with laminar flames in a constant pressure configuration. Gutkowski et al. [1] performed experiments with a square cross-section channel constructed of aluminum, studying the effect of channel width and equivalence ratio on flame speed, flame shape, and quenching. Dubey et al. [9] measured significant effects of thermoacoustic instabilities on flame shapes, speeds, and acoustic pressures generated in an 8-mm-diameter acrylic tube at atmospheric pressure. However, the effect of wall material thermal properties on the flame structure has not been explored. In the present study, the thermoacoustic response of ethylene-air flames propagating in narrow rectangular channels was experimentally explored by varying the channel width between 2.5 and 18 mm, the equivalence ratio of the ethylene-air mixture, and the channel wall material between acrylic, aluminum, and glass.

## 2 Experimental Setup

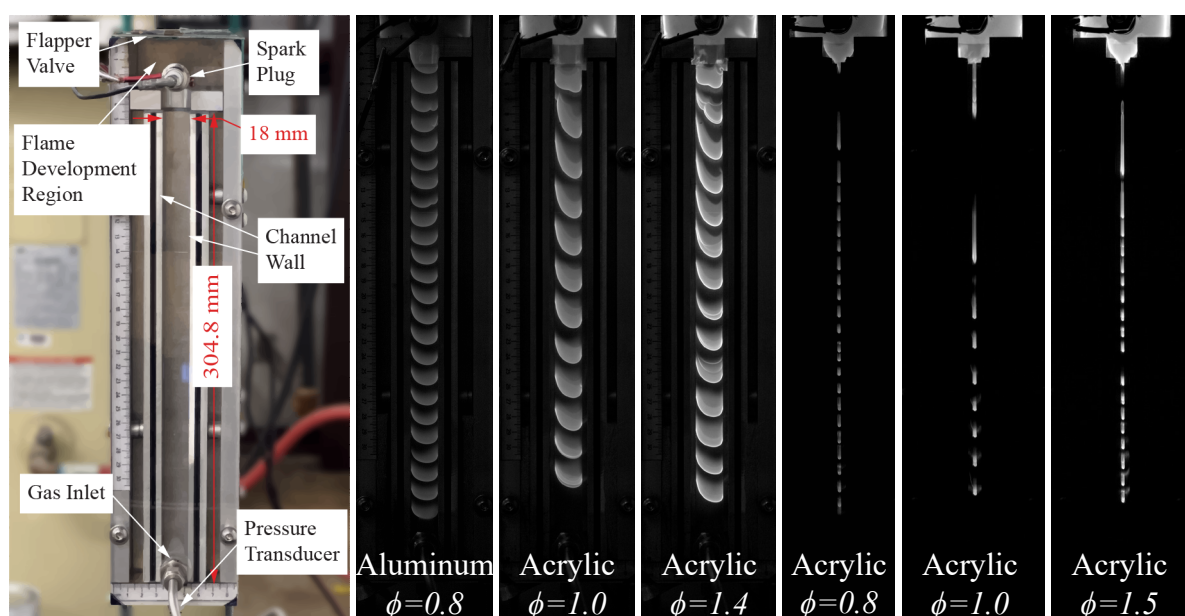


Figure 1: The experimental assembly (left) and flames in the 18-mm and 2.5-mm channel (right).

The experimental assembly (Fig. 1) was designed with an open ignition end and a closed propagation end in similar manner to the prior work of Gutkowski et al. [1]. It was composed of aluminum and acrylic (PMMA) to form a channel that was 305 mm long. The channel depth was 25.4 mm and the width was able to be varied with the use of standoffs. Channel widths of 18 mm and 2.5 mm were investigated in the present experiments. The effect of the wall composition on the 18-mm or 2.5-mm  $\times$  305-mm faces was also varied. The base material was aluminum, but thin (3.2 mm) strips of acrylic and glass were adhered to the aluminum substrate for some tests. The thermal conductivities for these materials varied by orders of magnitude as summarized in Table 1. The channels were sealed along all surfaces except for the top using o-ring cord and gasketing. The acrylic window contained a gas fill port at its bottom and also provided optical access to the channel. Combustion chemiluminescence was imaged with a high-speed camera (Phantom V2640) at 400 frames per second with a resolution of 4.9 px/mm. The bottom of the test channel was also fitted with a piezoelectric pressure transducer (PCB 102A15) sampled at 20 KHz.

Material	Thermal Conductivity (W/(m·K))	Heat Capacity (J/(kg·K))	Thermal Diffusivity (m <sup>2</sup> /s)	$b$ from [6]
PMMA	0.192	1420	$1.15 \times 10^{-7}$	0.354–1.37
Aluminum	237	903	$97.1 \times 10^{-6}$	519–2130
Glass	1.40	750	$7.47 \times 10^{-7}$	1.86–7.21

Table 1: Wall thermal conductivity, constant-pressure heat capacity, and thermal diffusivity from [10, 11]. Heat transfer transfer parameter  $b$  is defined below and is from [6].

The channel opened into an ignition volume that contained a spark plug which was driven by a coil-on-plug ignition coil. The ignition volume had dimensions of 63.5 mm wide  $\times$  63.5 mm deep  $\times$  76.2 mm tall and was covered by a 25.9-g and 1.5-mm-thick aluminum sheet, which served to contain the reactant gases before ignition. The generation of overpressure caused the lightweight sheet to lift and relieve the pressure, generating constant pressure combustion near atmospheric pressure  $P_a$ .

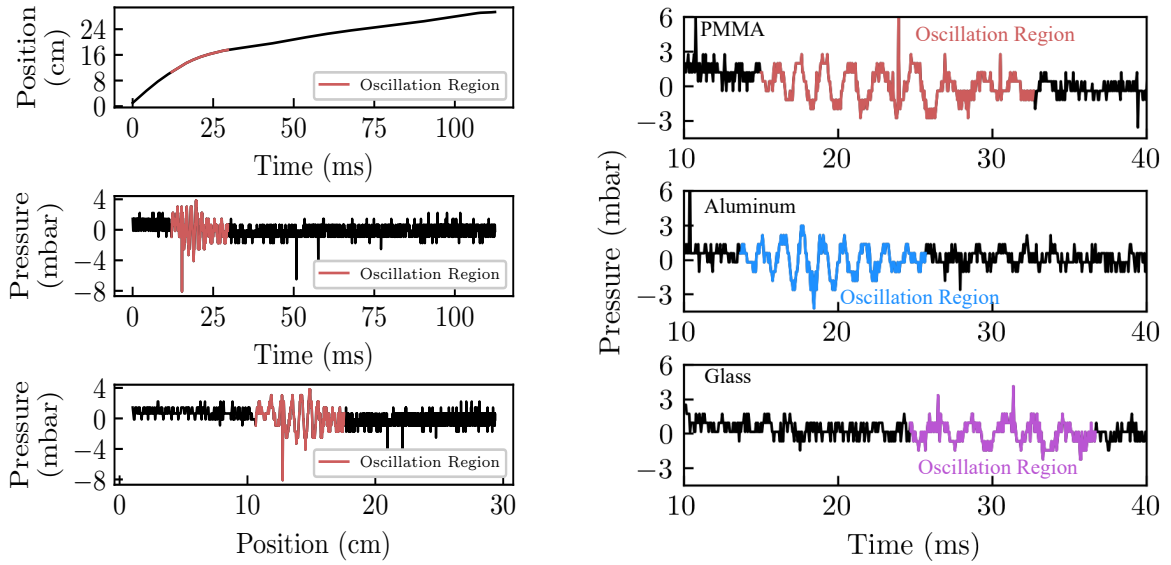
Mass flow controllers (Alicat Scientific MCP series) were used to vary the equivalence ratio  $\phi$  of the ethylene-air mixtures. The fill process was automated and injected a volume of reactant gas that, at atmospheric pressure, was equivalent to ten times the internal volume of the experimental assembly for each experiment. This was found to be sufficient to clear any prior air or products from the channel. During injection, the gases flowed through a 1-m-long, 12.7-mm-diameter tube filled with steel wool to promote turbulent mixing.

### 3 Results

Flames were successfully initiated for  $0.65 < \phi < 1.90$  in the ignition volume before transiting into the narrow channel. All flames in the 18-mm channel propagated its entire length. In the 2.5-mm channel, mid-channel quenching was observed outside of  $0.65 < \phi < 1.70$ . Flames appeared laminar after entering the channel and flame profiles from tests are in Fig. 1. Flame shapes in the 2.5-mm-wide channel appeared symmetric within the experimental resolution. Both symmetric and asymmetric shapes were observed in the 18-mm channel. The flame would switch between these two shapes for some tests. The flame location was identified by selecting the peak intensity pixel in the channel center for each image to generate position-time plots as shown at the top of Fig. 2a. The flame was unsteady upon entering the channel and rapidly decelerated to a steady speed that averaged twice the laminar flame speed. This deceleration was attributed to the flame adapting to the narrow channel confinement, which had higher heat and viscous losses when compared to the ignition volume. The flame speed measurements and the deceleration behavior are discussed in more detail in Ref. [2, 12].

Pressure measurements verified that the combustion remained at constant pressure and only detected acoustic effects in experiments with the 2.5-mm wide channel for  $1.05 < \phi < 1.35$ . Pressure oscillations only occurred over short lengths of the channel (2–7 cm) for short periods of time (6–20 ms). The majority of the pressure perturbations began in the unsteady region and damped after the flame transitioned to an approximately steady-state velocity (Fig. 2a). In some cases, however, the oscillations developed and decayed entirely within the steady region.

The amplitudes and periods of the acoustic waves were not constant for a given mixture. For equivalence ratios between 1.10 and 1.25, the pressure amplitude increased until reaching a maximum (Fig. 3b), then decreased as the pressure waves were damped. Maximum amplitudes occurred between  $1.20 < \phi < 1.25$  for all wall materials. A peak pressure of 5.7 mbar occurred in the acrylic channel (Fig. 2b), while peaks of 3.8 mbar were measured in both the aluminum and glass channels. The acoustic perturbations



(a) Flame deceleration and acoustics in acrylic for  $\phi = 1.2$ .

(b) Acoustic perturbations in the different wall materials at  $\phi = 1.25$ .

Figure 2: Acoustic wave development in the 2.5-mm-wide channel.

would initially grow in amplitude and then decay as shown in Fig. 2. The growth duration was approximately equal to the decay time (Fig. 3a) and the maximum amplitude (Fig. 3b) was nearly in the middle of the oscillation regime. This behavior was observed across all channel configurations. Outside of this equivalence ratio range, the pressure amplitude was generally small and approximately constant ( $P \approx 1.6$  mbar).

The acoustic frequency varied between 500 – 850 Hz across all tests. The acrylic tests generated frequencies between 538 – 750 Hz that monotonically increased with  $\phi$ . Frequencies in the aluminum and glass channels did not appear to correlate with  $\phi$ . The fastest oscillation within the aluminum channel had a frequency of 848 Hz for  $\phi = 1.2$  and the minimum frequency was 727 Hz corresponding to  $\phi = 1.15$ . Similarly, the glass-walled channel had frequencies ranging from 521 Hz ( $\phi = 1.15$ ) to 833 Hz ( $\phi = 1.1$ ).

#### 4 Discussion

Jiménez et al. [5, 6] observed the development of acoustic oscillations during regions of flame acceleration and deceleration. The largest oscillations were observed when flames were symmetric and heat losses were significant as summarized in Figs. 3 and 4 in Ref. [6]. Heat losses were represented by the parameter  $b = \frac{\lambda_{wall}}{\lambda_{gas}} \frac{\delta T}{t_{wall}}$  where  $\lambda$  is the thermal conductivity of the wall or gas,  $\delta T$  is the flame thickness and  $t_{wall}$  is the thickness of the conductive wall. The largest amplitude pressure oscillations were calculated at  $b = 0.05$ , with decreasing amplitudes at higher values of  $b$  [6]. In the present study, the flame thickness for the ethylene-air flames was predicted via Cantera [13] to calculate values of  $b$  for each wall material as listed in Table 1. The values of  $b$  are listed in Table 1. The flame thickness and thus  $b$  varied with  $\phi$ , yielding  $0.354 < b < 1.37$  for PMMA, followed by  $1.86 < b < 7.21$  for glass, and  $519 < b < 2130$  for aluminum.

The most similar heat loss parameters that Jiménez et al. [6] explored were  $b = 0.1$  and  $b = 1$ , which were comparable to the acrylic and the glass-walled channels, respectively, in the present study. The aluminum  $b$  value for the present experiments was outside the range studied by Jiménez et al. [6]. The

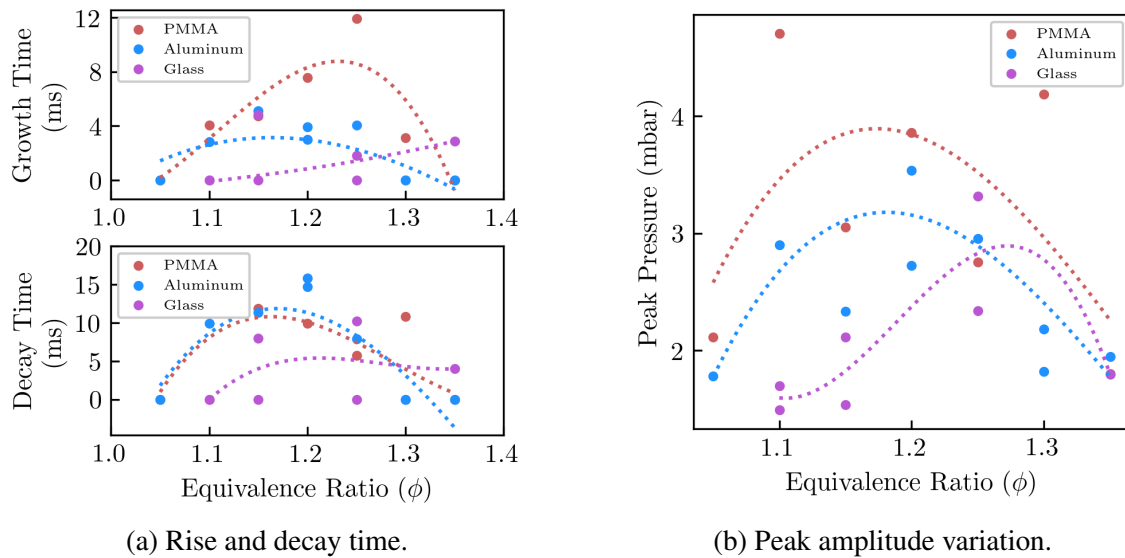


Figure 3: Variation in acoustic effects with wall material and  $\phi$ , with curves showing trends.

peak amplitude oscillations were calculated [6] to occur for  $b = 0.1$ , which is consistent with these experimental results. The amplitude of the acoustic pressure oscillations in Ref. [6] varied with flame shape and channel dimensions, but ranged from  $0.02$ – $0.05 P_a$ , while the experimental oscillation amplitudes were one order of magnitude smaller at  $0.005 P_a$ .

Jiménez et al [5, 6] also identified a critical channel thickness above which symmetric flames would become asymmetric. This thickness was  $17\delta_T$  for their specific parameters that were intended to model fuel–air systems. In the present experiments, unstable flame shapes were sometimes observed in the 18-mm channel and not in the 2.5-mm channel, which is consistent with the concept of a critical minimum channel width to preserve flame symmetry [5, 14]. Jiménez et al. [5] also noted that asymmetric flames within wider channels tended to produce weak or negligible acoustic waves when compared to symmetric flames. In addition to not supporting flame asymmetry, the larger channels would also reduce the relative effects of wall heat losses on the flame.

Finally, it is important to note that only two of the walls contacting the flame were composed of the wall material of interest in the present experiments. One of the remaining walls was composed of aluminum and the other of acrylic. This would likely introduce some asymmetry to the flame in the viewing direction and also reduce the effect of the varied wall material on the flame properties.

## 5 Conclusion

The thermoacoustic response of ethylene-air flames in narrow rectangular channels was explored with the wall conductivity, channel width, and equivalence ratio as independent variables. Flames were symmetric for the narrow channel width and both symmetric and asymmetric for the wider channel tested. Thermoacoustic pressure oscillations were observed in the 2.5-mm channel when  $1.00 < \phi < 1.35$  and the flame was accelerating. The strongest pressure oscillations occurred for acrylic walls, while slightly weaker amplitude ones were observed for aluminum and glass walls. These results were consistent with prior numerical work [6] and support predictions that variations in wall conductivity can affect the development of the thermoacoustic instability for combustion waves transiting in the long-aspect-ratio channels.

**References**

- [1] A. Gutkowski, L. Tecce, and J. Jarosinski, “Some features of propane-air flames under quenching conditions in narrow channels,” *Combustion Science and Technology*, vol. 180, pp. 1772–1787, 2008.
- [2] Z. Negrette, S. Jackson, and M. Short, “An experimental investigation of ethylene-air flames propagating in narrow rectangular channels,” in *AIAA SCITECH 2024 Forum*, 2025, pp. 10.2514/6.2024–2025.
- [3] W. B. Howard, “Flame arresters and flashback preventers,” *Plant/Operations Progress*, vol. 1, no. 4, pp. 203–208, 1982.
- [4] A. C. Fernandez-Pello, “Micropower generation using combustion: Issues and approaches,” *Proceedings of the Combustion Institute*, vol. 29, no. 1, pp. 883–899, 2002.
- [5] C. Jiménez, D. Fernández-Galisteo, and V. N. Kurdyumov, “Flame-acoustics interaction for symmetric and non-symmetric flames propagating in a narrow duct from an open to a closed end,” *Combustion and Flame*, vol. 225, pp. 499–512, 2020.
- [6] C. Jiménez and V. N. Kurdyumov, “Flame-acoustics interaction for flames propagating from the open to the closed end of a channel: Effects of heat losses and the lewis number,” *Combustion and Flame*, vol. 246, p. 112371, 2022.
- [7] V. N. Kurdyumov and C. Jiménez, “Propagation of symmetric and non-symmetric premixed flames in narrow channels: Influence of conductive heat-losses,” *Combustion and Flame*, vol. 161, no. 4, pp. 927–936, 2013.
- [8] M. Gonzalez, R. Borghi, and A. Saouab, “Interaction of a flame front with its self-generated flow in an enclosure: The “tulip flame” phenomenon,” *Combustion and Flame*, vol. 88, pp. 201–220, 1992.
- [9] A. Dubey, Y. Koyama, N. Hashimoto, and O. Fujita, “Acoustic parametric instability, its suppression and a beating instability in a mesoscale combustion tube,” *Combustion and flame*, vol. 228, pp. 277–291, 2021.
- [10] M. Assael, S. Botsios, K. Gialou, and I. N. Metaxa, “Thermal conductivity of polymethyl methacrylate (PMMA) and borosilicate crown glass BK7,” *International Journal of Thermophysics*, vol. 26, pp. 1595–1605, 2005.
- [11] T. Bergman, A. Lavine, F. Incropera, and D. DeWitt, *Fundamentals of Heat and Mass Transfer, 7th Ed.*, 8th ed. John Wiley & Sons, 2017.
- [12] Z. Negrette, S. Jackson, and M. Short, “The influence of channel width and thermal conductivity on flame propagation in ethylene-air mixtures,” in *Proceedings of the 14th United States National Combustion Meeting*, 2025.
- [13] D. G. Goodwin, R. L. Speth, H. K. Moffat, and B. W. Weber, “Cantera: An object-oriented software toolkit for chemical kinetics, thermodynamics, and transport processes,” <https://www.cantera.org>, 2021, version 2.5.1.
- [14] C. H. Tsai, “The asymmetric behavior of steady laminar flame propagation in ducts,” *Combustion Science and Technology*, vol. 180, no. 3, pp. 533–545, 2008.